GlennICE 2.1 Capabilities and Results

Wright, William B.[1]
HX5, LLC, Cleveland, OH, 44135, USA

Christopher. E. Porter[2]
NASA Glenn Research Center, Cleveland, OH, 44135, USA

Eric T. Galloway [3] and David L. Rigby [4]
HX5, LLC, Cleveland, OH, 44135, USA

GlennICE (Glenn Icing Computational Environment) is a computational tool designed to calculate ice growth on complex three-dimensional geometries using the input from a user-supplied computational fluid dynamics (CFD) solution for the geometry of interest. The NASA John H. Glenn Research Center at Lewis Field is developing this tool to aid those evaluating, designing and certifying aircraft, engines, and aircraft components for flight in icing conditions. This domestically available software is being developed to enable the introduction of new icing physics into a computational environment in a manner that is open for evaluation and eventual use by industry, academia, and other government organizations. This paper will document the current capabilities for version 2.1 of this software and provide example cases with comparison to available experimental data.

I. Nomenclature

A	augmentation constant, dimensionless
AOA	angle of attack, deg
C_p	pressure coefficient, dimensionless
htc	heat transfer coefficient, W/m^2K
htc_A	augmented heat transfer coefficient, W/m^2K
R_q	roughness Height, m
ΔT_{os}	temperature difference (freezing temperature – total temperature), K
LWC	liquid water content, g/m^3
MVD	median volume diameter, microns
P	static pressure, Pa
T	static temperature, °C
time	time, s
t_r	rime thickness, m
$t_{r,max}$	maximum ideal rime limit
x	x-direction, m
x_rot	x-direction after rotation by sweep angle, m
y	y-direction, m
z	z-direction, m
V_∞	freestream velocity, m/s
β	collection efficiency, dimensionless
η	freezing fraction, dimensionless
ρ_{ice}	ice density, kg/m^3

II. Introduction

A research project is underway at the NASA Glenn Research Center (GRC) to produce computer software that can accurately predict ice growth under any meteorological conditions for any aircraft surface. The Icing Branch at GRC has previously produced computer software [1] [2] over the last thirty years for performing icing simulation.

[1] Research Engineer, Icing Branch, Senior Member AIAA.
[2] Research Engineer, Icing Branch, Member AIAA
[3] Software Engineer, Icing Branch
[4] Research Engineer, Icing Branch, Member AIAA

While some of these tools have been collaborative projects, most have been developed primarily by one person with some assistance by others. The state of computing has also changed dramatically in that time period. Early on, design decisions were made in these tools that took into consideration the limited capabilities of early computers. Additionally, the personnel tasked to design and write this software were icing experts, not software experts. As these codes have grown in complexity and have been accepted by users as production icing tools, there has arisen a need for the developers to adhere to standard software practices used to develop commercial software. The goals of these practices, as they relate to the GlennICE effort, include creating a team-based development process rather than the previous individual-based process; building modular code elements that can be re-used as needed by several processes; designing or redesigning code elements with future capabilities in mind; and developing efficient testing methodologies for testing and validation of the code. This report will, in part, provide an update on the status of that process and describe the current capabilities of the GlennICE.

For those readers familiar with NASA's other computational icing tools, LEWICE [1] and LEWICE3D [2], they should note that GlennICE is being designed to address a generalized three-dimensional icing problem. This differs from LEWICE and LEWICE3D, both of which relied on assumptions that are well suited for performing analysis on special cases, such as cantilevered wings, but not necessarily the optimal approach for the general case. As such, GlennICE is at a lower Technology Readiness Level (TRL) [3] than LEWICE and LEWICE3D for these special cases. Future versions of the software are planned to be completed on a regular basis and will include the improvements and validation necessary to mature the software to a comparable TRL. As such, this version of GlennICE is currently a research tool rather than a design or certification tool.

GlennICE is also a completely new software that is being developed with modern software practices. Because of this, legacy routines from LEWICE3D are not being used. However, it calculates water collection on a surface using the Lagrangian reference frame as did LEWICE3D. Recent research in icing has seen the development of several tools that perform these calculations in the Eulerian reference [4][5][6]. Each method has advantages in its favor. Eulerian algorithms are easier to develop as many of the routines can be leveraged from the flow solver and can be solved as a coupled system in order to compute evaporation and sublimation effects which are important inside the engine. They can solve time accurate solutions more simply than Lagrangian systems. Eulerian calculations are typically computationally faster [7] than Lagrangian methods and provide particle concentrations throughout the domain. However, the Lagrangian reference frame is more physically accurate, since the particle flow may not represent a continuum. This is especially true for secondary particle flows such as splashing and breakup. A Lagrangian routine can more easily use flow solutions from any CFD solver. They are also better at capturing gradients in the particle flow. Eulerian systems typically use the same grid for the flow solution and the particle flow. A grid that is designed to capture gradients in the air flow cannot also capture large gradients in the water flow unless a more refined grid is used, which reduces the computational advantage of the Eulerian system. This paper will present the process used for calculating ice shapes.

III. Methodology

This section is intended to describe the workflow of an initial GlennICE run to aid the user in becoming familiar with the GlennICE software. The complete workflow for the GlennICE software is illustrated in Figure 1. The white boxes in the process are external to GlennICE and accomplished with third party software. The green, blue, red, and orange boxes denote work accomplished by the GlennICE software.

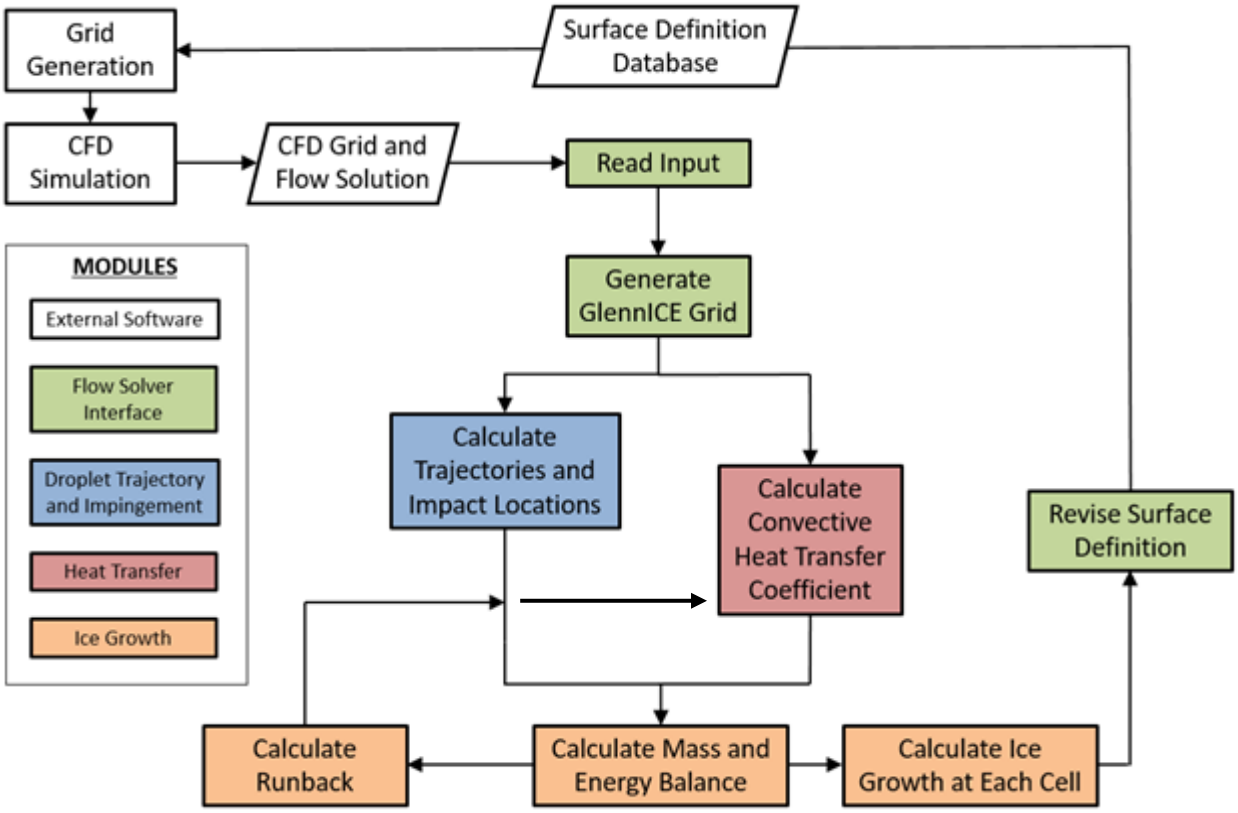

Figure 1. Flow chart of the GlennICE process.

This flow chart illustrates a multi-shot simulation strategy where the user is responsible for remeshing the new iced geometry and rerunning the Computational Fluid Dynamics (CFD) solver. This multi-shot capability is optional, and currently only single shot computations have been performed.

CFD Solver Requirements

GlennICE uses a discretized flow field generated from a Computation Fluid Dynamics (CFD) solver. To maintain flexibility with a wide variety of commercial and in-house CFD solvers, the coupling between GlennICE and the CFD software is currently all one-way coupling. As such GlennICE can be classified as a CFD post-processor. Currently this level of coupling has been sufficient for external icing problems. Because of the one-way coupling, GlennICE can theoretically accept solutions from a wide variety of CFD solvers. It does this by supporting a handful of widely used CFD file formats that a majority of CFD solvers utilize. However, it should be noted that there are many storage variants. GlennICE requires pressure, density the three velocity components and the three components of the surface wall shear. It also requires the estimated wall distance to the surface which was used by the turbulence model and either the heat transfer coefficient or the wall heat flux and wall temperature. Currently GlennICE will read solutions in Fieldview [8] unstructured format or Tecplot [9] szplt format.

Particle Trajectories

GlennICE integrates particle trajectories using a method developed by Dormand and Prince [10]. It is a 4^{th} order Runge-Kutta scheme that is designed to minimize error of the 5^{th} order term. This means that it computes both the fifth order result and the 4^{th} order result and returns the difference as the error. The algorithm was developed by Hairer et. al.[11] and is the default integrator used by MATLAB [12] and GNU Octave [13]. The interface between the

DOPRI5 routines and GlennICE resides in a subroutine that contains the derivative function, which in this case is the equation of motion in the Lagrangian reference frame. Particles are released from a user-supplied bounding box and subsequently refined based on the distance of the trajectory to the surface or based on whether it hits. Details of this method were presented previously[14]. It is important to note that particle physics such as splashing [15], breakup [16] as well as energy and mass transport to and from particles in transit to the surface [16] [16] which were part of the LEWICE2D/3D or TADICE process have yet to be implemented in the current version. It should also be noted that the GlennICE in reference 16 refers to a modularized version of LEWICE (2D) and not the current development process.

Heat Transfer Coefficient

Heat transfer coefficients can be specified using either a single CFD solution or two solutions. The single solution methodology assumes the CFD solver provided a value of heat transfer coefficient. Alternatively, the user can provide GlennICE with two CFD solutions differing only by the wall thermal boundary condition. GlennICE uses this information to calculate heat transfer coefficient and adiabatic wall temperature. It is assumed that the heat transfer coefficient, htc, and adiabatic wall temperature, T_{aw}, are independent of wall thermal condition. Therefore, at every location, given (T_1,q_1) and (T_2,q_2) two simultaneous equations are solved for htc and Taw. This technique relies on the definition of htc from the equation: $q = htc * (T_{wall} - T_{aw})$. The user can specify these two files if they consist of identical meshes, however, the two CFD solutions differ in their specification of the temperature of the surface. These options do not necessarily account for the roughness effects, however. Many solvers contain a turbulence model that accounts for sand-grain roughness such as those proposed in references [18]-[26]. In lieu of this, the heat transfer coefficient computed by this process was augmented using an empirical roughness model that was developed by McClain [27] to predict roughness variation on a surface. The equations programmed into GlennICE are shown below. These equations use two user-defined values that can be adjusted. The first user-defined value is the ideal rime limit, $t_{r,max}$ and the second empirical constant is the augmentation constant, A. The McClain paper only provides equation [1] and does not define $t_{r,max}$ or the heat transfer augmentation. The best values for these parameters are the subject of ongoing research. The values selected for this paper were chosen to provide the best fit to the experimental data.

Since this equation depends on freezing fraction, which depends on the heat transfer coefficient chosen, an iterative approach was used to find final values. The initial heat transfer coefficient was used to find a freezing fraction at each face. Then that freezing fraction was used to find the roughness and augmented heat transfer coefficient for each face as shown below. The second iteration would then use the updated heat transfer coefficient and the process would continue until values no longer change. Typically, six iterations have proven sufficient to converge to the final heat transfer coefficient.

$$R_q = t_r 0.7(1 - C_p)\eta \left(0.34 + \Delta T_{oS}^{2/3} exp\left[-\frac{\Delta T_{oS}}{2.25}\right]\right) \quad [1]$$

Where

$$t_r = min\left[\frac{LWC * V_\infty * time * \beta}{\rho_{ice}}, t_{r,max}\right] \quad [2]$$

The augmented heat transfer is

$$htc_A = htc * \left(1 + A\frac{R_q}{0.001}\right) \quad [3]$$

A and $t_{r,max}$ are the user-defined parameters described above. A linear expression relating roughness to heat transfer coefficient was chosen for simplicity. Other forms of augmentation could be used in the future.

Surface Mass/Energy Balance

The mass and energy balance at the surface uses the same terms as employed in LEWICE. However, LEWICE required a marching algorithm starting at a stagnation point to compute the runback ice mass. To avoid this, GlennICE uses the surface shear stress from the CFD solver. There are four ways that water flow can enter or exit a triangular surface face. These are depicted in Figure 2. If the flow is exactly parallel to any face, that simplifies the analysis but does not change that there are four flow types. Figure 2a shows flow out all edges. This would be equivalent to a stagnation point flow such as LEWICE but the current scheme does not require that such a face exists nor would the simulation start at that face if it did exist. Figure 2b shows flow in through one edge and out the other two. Figure 2c shows flow in through two edges and out the third edge. Figure 2d shows a case where there is only flow into a face.

This has occurred on some wing geometries where there is flow in from two faces and the third edge has no flow out since it is on a boundary. The direction of water flow is determined by the shear stress vector as shown in Figure 3.

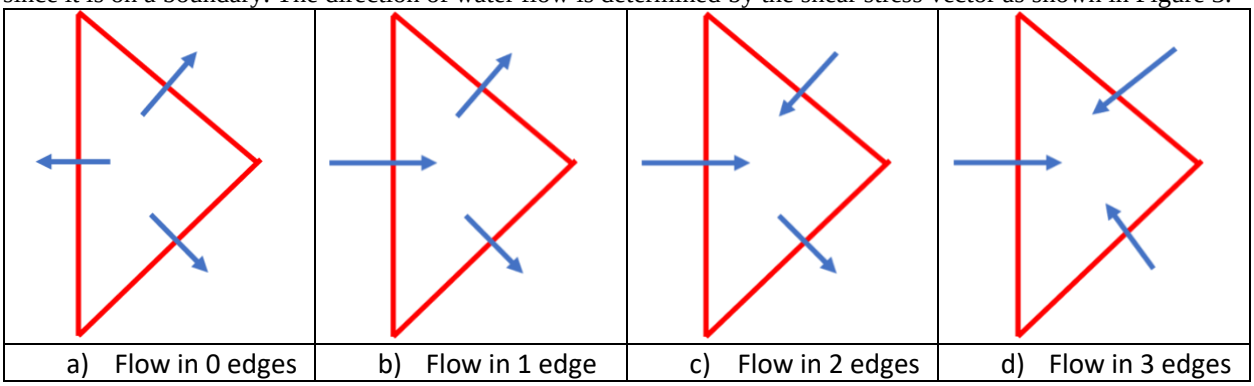

Figure 2 Runback Water Flow Types

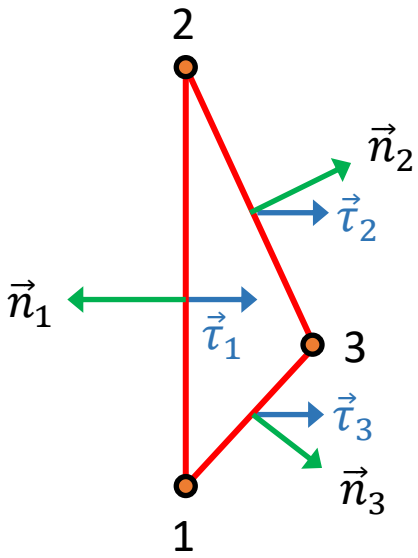

Figure 3 Runback Flow Direction from a Single Surface Face

The solution for the final runback and refreezing through the domain is iterative. On the first iteration, the amount of ice formed is computed at each face from the amount that impinged and the energy balance. GlennICE will also determine the maximum amount of ice that could freeze at this face, called the mass potential. For example, if the mass impinged on a face is equal to 1 unit and the amount that can freeze is 0.5 units, there is 0.5 units of mass available to runback and the leftover mass potential is zero for this face. However, if the mass impinged is 1unit and the face could freeze 1.5 units of mass, then all the impinging mass freezes on this face and the face could freeze an additional 0.5 units if it receives any runback water. If a face has more water than it can freeze, the surface shear stress vector determines the surface edge(s) it will flow out from and the amount of water exiting each edge. The shear stress is provided by the flow solution at the nodes and the values at the edge center shown in the diagram are calculated. The total mass flow in will equal the mass flow out minus the additional freezing that takes place. For Figure 2b, where the flow goes in one edge and out the other two edges, the mass flow out the two edges will be proportional to the shear stress. For example, if the flow in edge 1 is 1 unit and the shear stress times the edge length through edge 2 is twice the value through edge 3, then the flow out edge 2 is 2/3 units and the flow out edge 3 is 1/3 units provided no water froze. On the first iteration, no water flows into any face. The amount of mass leaving is calculated. Between the first and second iterations, the runback mass out each face is moved to the next face as described above. On the second iteration, the mass of water entering a face is compared to the available mass potential. If all the water entering the face freezes, nothing else need to be done. If there is more water entering the face than can freeze, the iterations will continue. This process assumes the energy contained in the runback water is negligible and that the icing time is

large enough for the runback water to reach any face on the surface. The equations are not time dependent and may not handle all situations such as recirculation of runback water. Models for these effects are part of ongoing research. Figure 4 shows the runback process described above for a single runback iteration. In each face, water either flows in one edge and out the other two or it flows in edges and out the remaining edge.

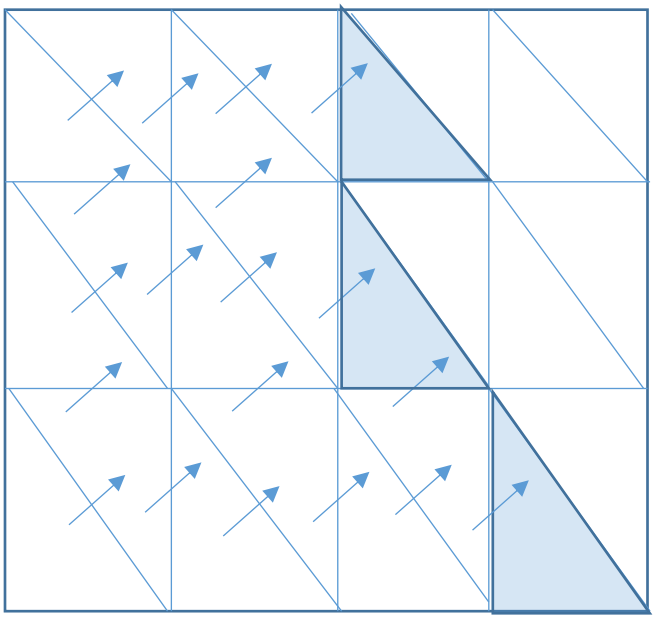

Figure 4 Water Runback for a Single Iteration (Freezing Front is Shaded)

Ice Growth (Surface Modification)

A fully three-dimensional ice growth was produced using a prismatoid method with node-based smoothing. The process is based on computing the node centered normal vectors and solving a cubic equation at each location to find the appropriate distance from the surface that maintains the computed ice volume. This surface redefinition process was described in a previous paper [28] and will not be replicated here.

IV. Results

Three cases were selected for comparison. The first case is a straight wing NACA0012 from the LEWICE validation database [29]. The second case is a straight wing NACA23012 from the 1st Ice Prediction Workshop [30]. The third case is a NACA0012 at 30° sweep and is also from the Ice Prediction Workshop. Table 1 shows the conditions for these cases.

Table 1 : Icing Conditions for Comparison Cases

Airfoil	Chord(m)	Sweep(deg)	AOA(deg)	V_∞(m/s)	T(°C)	P(Pa)	LWC(g/m3)	MVD(μm)	time(min)
NACA0012	0.5335	0	4	66.88	-4.5	98440	1.0	20	6
NACA23012	0.4572	0	2	102.88	-7.1	92941	0.83	15	5
NACA0012	0.9144	30	0	115	-10	90321	0.5	20.5	17.7

Section IV.1: NACA0012 Case

The first geometry simulated is a straight wing NACA0012 with a chord length of 0.5334 m (21") with a far-field boundary approximately 20 chord lengths upstream and downstream of the wing. The outer block of the domain is a hexahedron. The top and bottom boundaries were also placed 20 chord lengths from the wing. The span of the wing was 0.9 m. Slip Wall boundaries were used on the sides, top and bottom of the domain. The minimum x boundary was designated the inlet with the maximum x-boundary was the outlet. The grid was generated in Pointwise [31] by creating an unstructured domain in 2D and extruding spanwise. The 2D unstructured grid used structured quads near the surface using the T-Rex function with a ∂s at the wall of $1.7e^{-6}$ to achieve a y+ <= 1. The wing section has a no slip wall boundary. The resulting 2D grid is shown in Figure 5. The final 3D grid consists of 35,194 tetrahedrons, 290,601 hexahedrons, 891 pyramids and 53,829 prisms for a total of 380,515 cells in the mixed element domain.

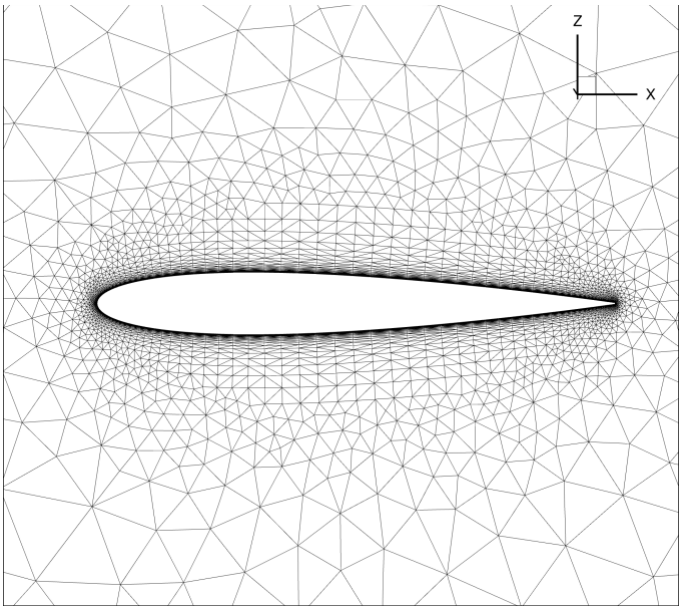

Figure 5 Mesh spacing (2D) after T-rex function utilized

The flow solution was performed using ANSYS-CFX [32] with a Shear Stress Transport turbulence model. Both flow solutions were generated using the following flow conditions: AOA = 4°, V_∞ = 66.88 m/s (130 knots), T = -4.5°C, P = 98440. The first flow solution used a constant wall temperature of 20°C and the second flow solution used a constant wall temperature of 30°C. The two different wall temperatures are used in GlennICE to compute the heat transfer coefficient. The icing conditions for this case were LWC = 1 g/m^3 a MVD size of 20 microns and a six (6) minute icing time. This case is part of the standard LEWICE validation database [29]. Figure 6 shows a contour plot of Mach number for this case while Figure 7 shows pressure. Figure 8 shows surface pressure coefficient on the NACA0012. Figure 9 shows collection efficiency for this case, while Figure 10 shows freezing fraction. In these plots, the span direction is y.

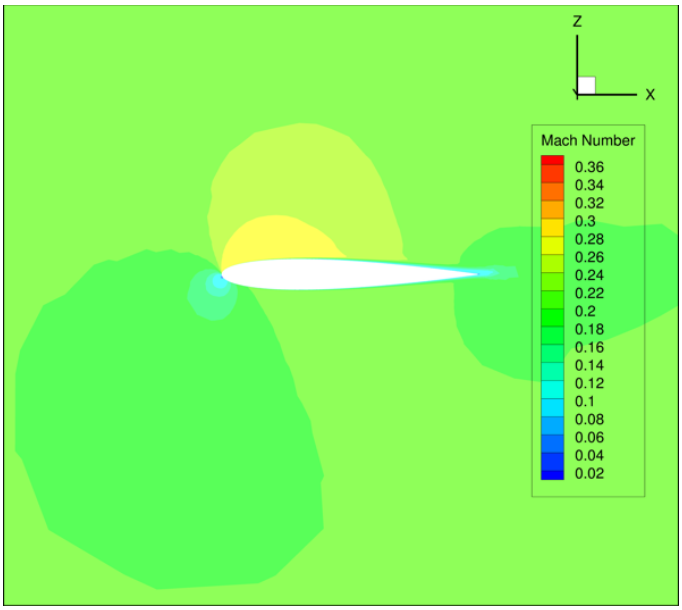

Figure 6 Mach Number Contour for Flow Solution

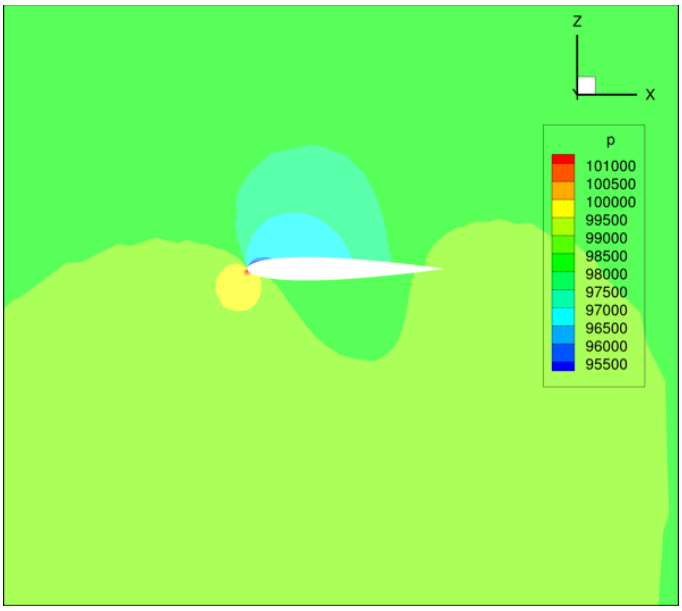

Figure 7 Pressure Contour for Flow Solution

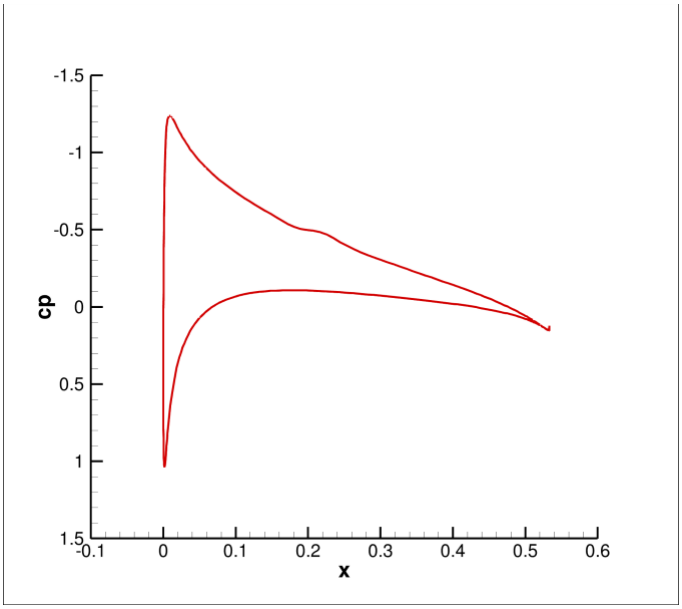

Figure 8 Pressure Coefficient for NACA0012 Case

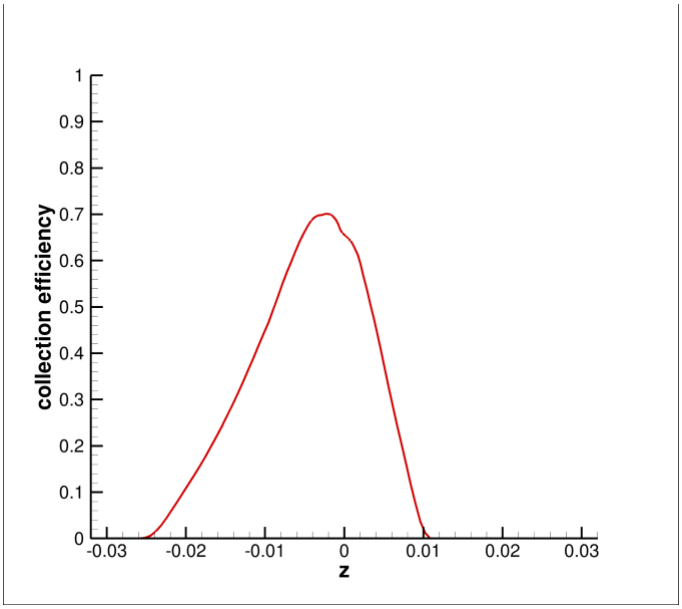

Figure 9 Collection Efficiency (β) for NACA0012 Case

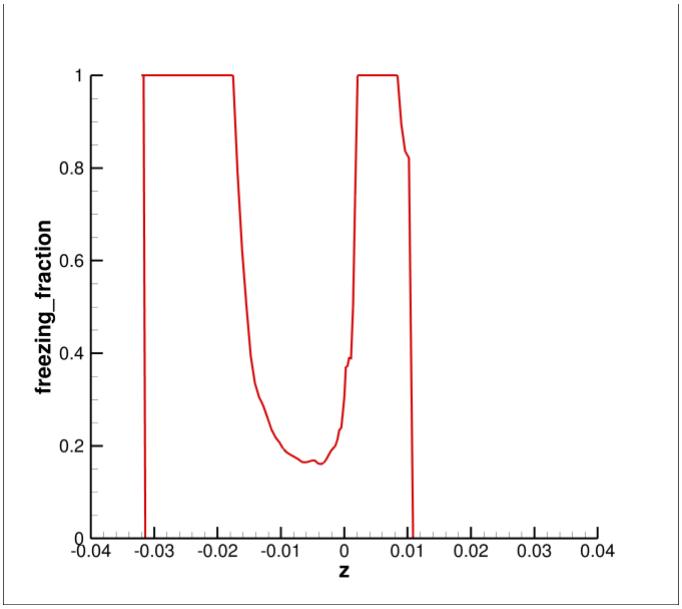

Figure 10 Freezing Fraction (η) for NACA0012 Case

This example case makes use of the new roughness model proposed by McClain [27]. The roughness distribution predicted is shown in Figure 11 and the associated augmentation (the ratio of htc_A/htc) is shown in Figure 12. The ideal rime limit in Equation (2) was $t_{r,max}$=0.004 m (4 mm) and the heat transfer augmentation in Equation (3) was A=2.

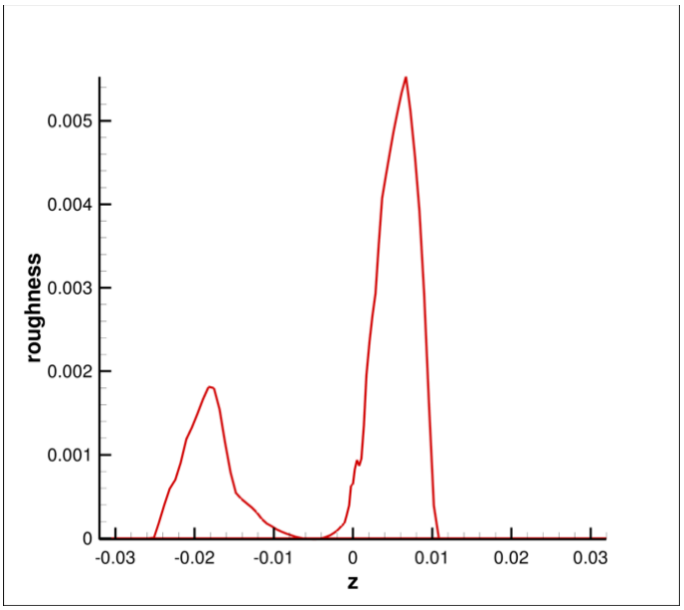

Figure 11 Roughness (R_q) Distribution Predicted for NACA0012 Case

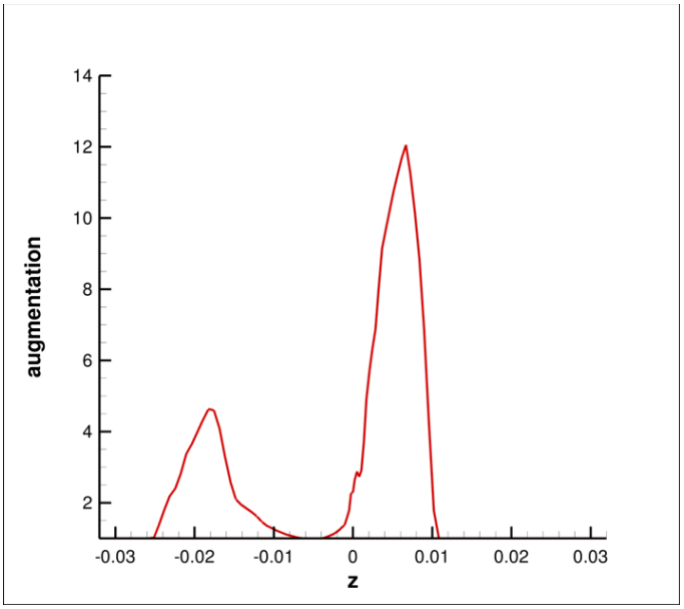

Figure 12 Heat Transfer Augmentation Ratio (htc_A/htc) for NACA0012 Case

Since the example case is two dimensional, and the conditions correspond to values from experiments conducted in the NASA Icing Research Tunnel (IRT) this geometry can be compared to the 2D tracing from that experiment. The comparison is shown in Figure 13.

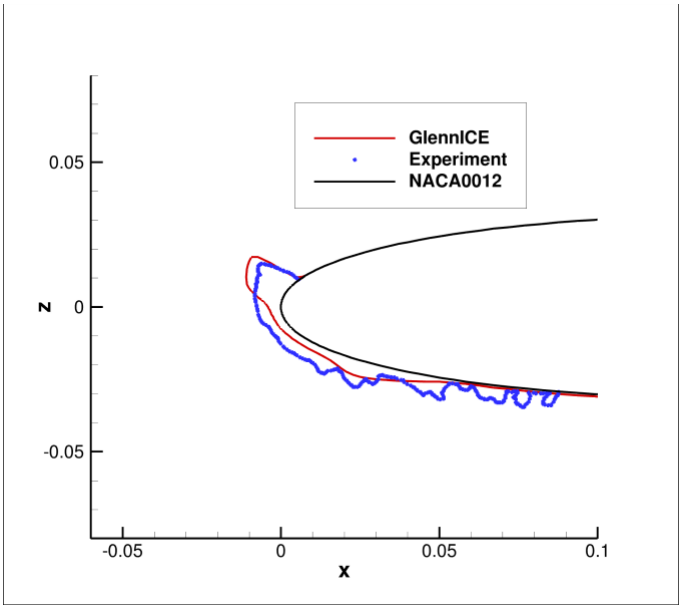

Figure 13 Comparison of GlennICE 2D Ice Accretion Profile to Experiment

Section IV.2: NACA23012 Case

The second case used for comparison comes from the 1st AIAA Ice prediction Workshop [30]. The case is a straight wing NACA23012 profile. In that workshop, the case was referenced as Case 242. The geometry has a chord length of 0.4572 m (18") with a far-field boundary approximately 3 meters upstream and downstream of the wing. The outer block of the domain is a hexahedron. The top and bottom boundaries were also placed 1.4 meters from the wing. The span of the wing was 2.7 m. Slip Wall boundaries were used on the sides, top and bottom of the domain. The minimum x boundary was designated the inlet with the maximum x-boundary was the outlet. The grid was supplied as part of the workshop. The grid was converted to tetrahedrons within GlennICE. The 2D grid profile is shown in Figure 14. The final 3D grid consists of 16,375,816 tetrahedrons and 6,009,480 points.

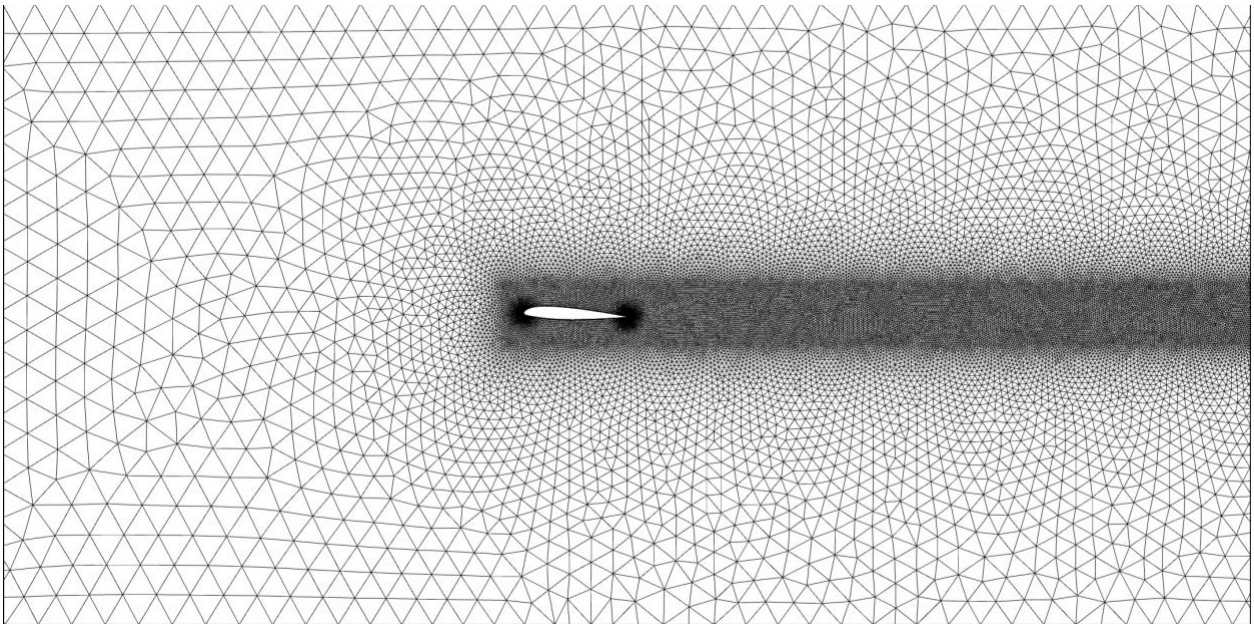

Figure 14 Grid profile for NACA23012 case

The flow solution was performed using FUN3D with a Shear Stress Transport turbulence model. Both flow solutions were generated used the following flow conditions: AOA = 2°, V_∞ = 102.88 m/s (200 knots), T = -7.1°C, P = 92941 Pa. The first flow solution used a constant wall temperature of 20°C and the second flow solution used a constant wall temperature of 30°C. The two different wall temperatures are used in GlennICE to compute the heat transfer coefficient. Icing conditions for this case are LWC=0.83 g/m3, MVD=15 microns and an icing time of five (5) minutes. Figure 15 shows a contour plot of Mach number for this case while Figure 16 shows pressure. Figure 17 shows surface pressure coefficients on the NACA23012 with comparison to experiment [30]. Figure 18 shows collection efficiency for this case. Figure 19 shows the freezing fraction calculated for this case. Figure 20 shows the roughness distribution predicted using an ideal rime limit ($t_{r,max}$= 0.008 m) while Figure 21 shows the associated heat transfer augmentation ratio (htc_A/htc) using an augmentation level (A=3). Figure 21 shows the ice shape generated which is compared to the ice shape traced from the experiment. In these plots, the span direction is z as that is how the data was provided in the workshop.

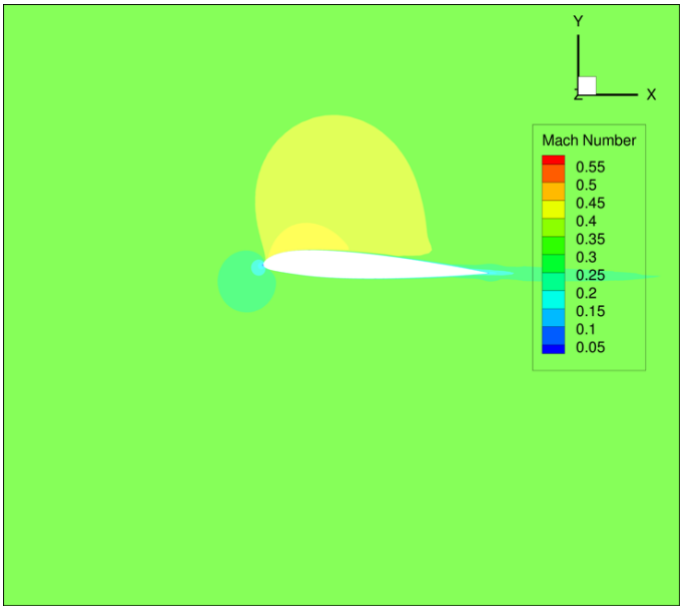

Figure 15 Mach Number for NACA23012 Case

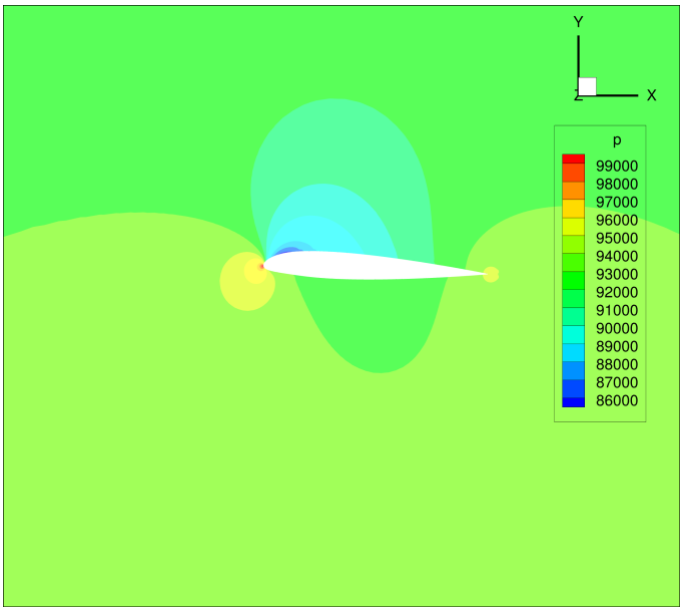

Figure 16 Pressure Contours for NACA23012 Case

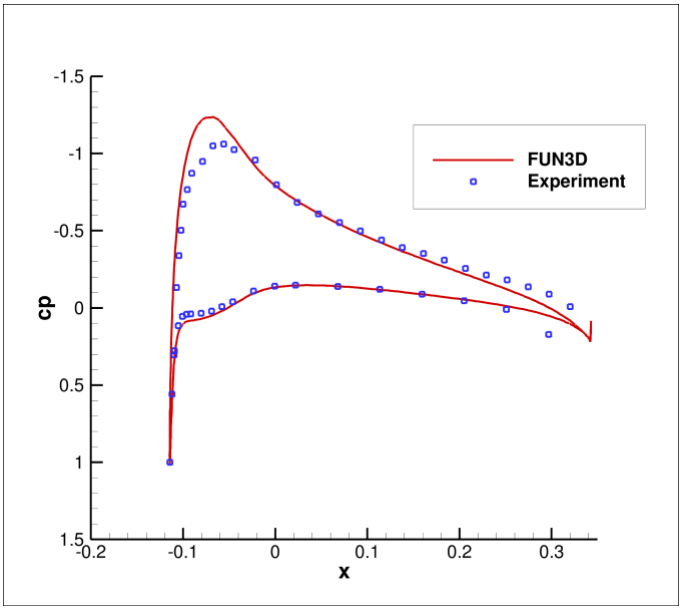

Figure 17 Pressure Coefficient for NACA23012 Case

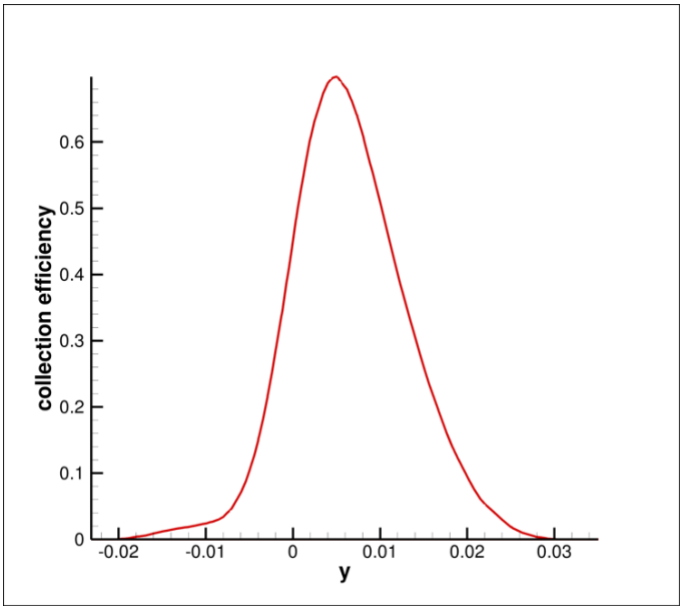

Figure 18 Collection Efficiency (β) for NACA23012 Case

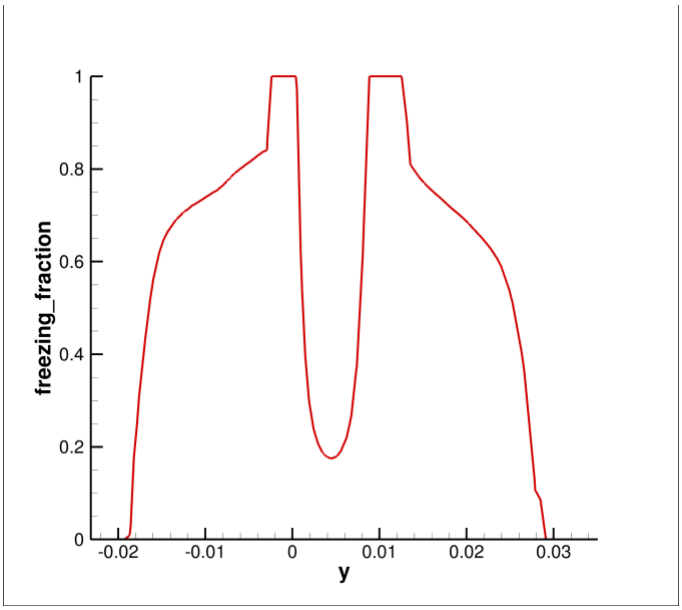

Figure 19 Freezing Fraction (η) for NACA23012 Case

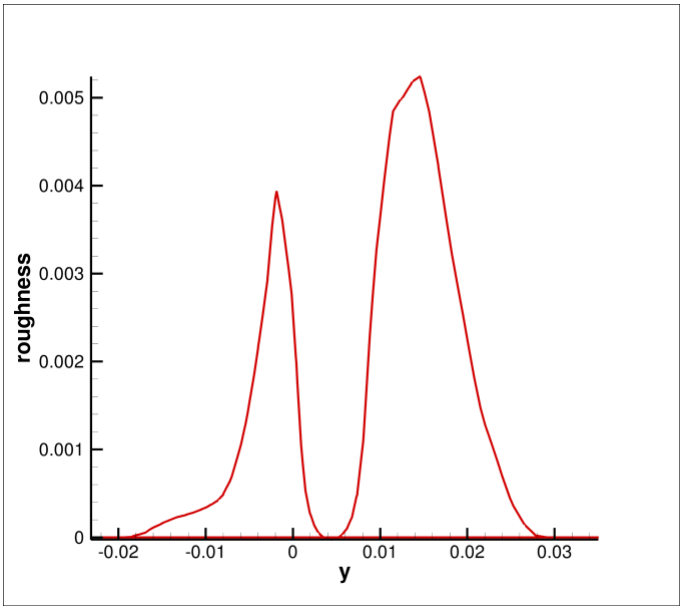

Figure 20 Roughness (R_q) Prediction for NACA23012 Case

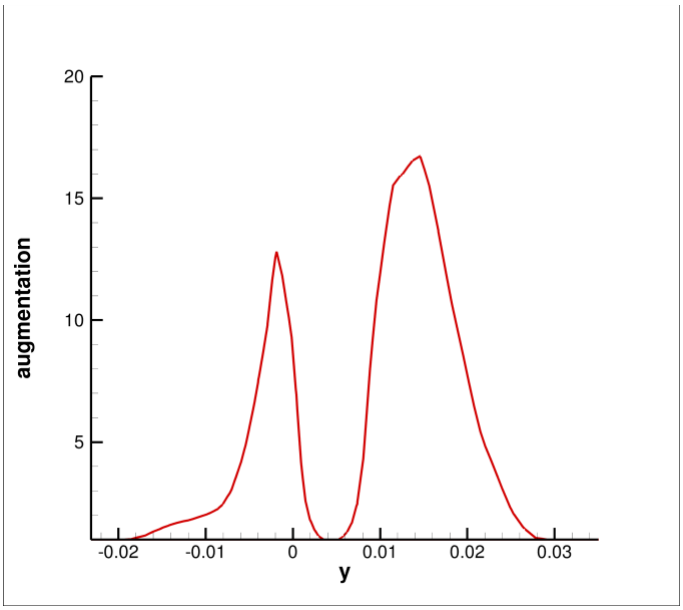

Figure 21 Heat Transfer Augmentation (htc_A/htc) for NACA23012 Case

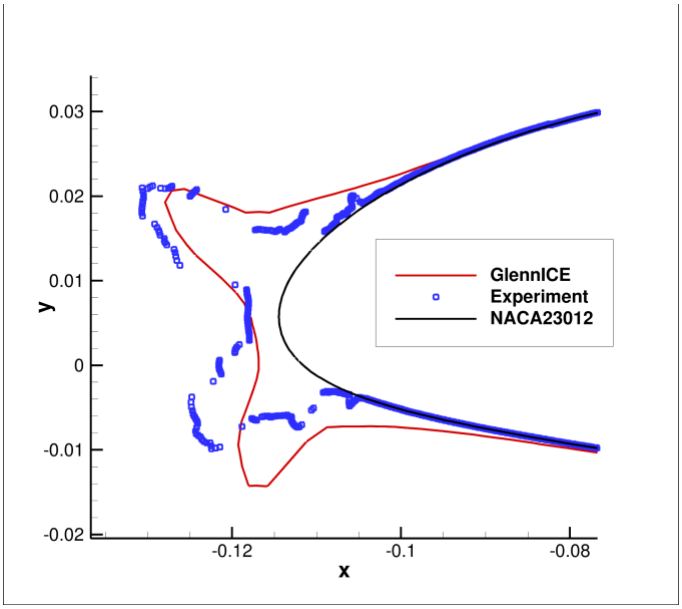

Figure 22 Ice Shape Prediction for NACA23012 Case

Section IV.3: Swept NACA0012 Case

While the two previous cases were computed in three dimensions, the geometries consist of two-dimensional airfoils extruded into the span direction. The final case was performed on a 3D NACA0012 wing at a 30° sweep angle and 0° AOA. This case also comes from the Ice Prediction Workshop and was called Case 363 in the workshop documentation. The geometry has a chord length of 0.9144 m (36") with a far-field boundary approximately 3 meters upstream and downstream of the wing. The outer block of the domain is a hexahedron. The top and bottom boundaries were also placed 1.4 meters from the wing. The span of the wing was 2.7 m. Slip Wall boundaries were used on the sides, top and bottom of the domain. The minimum x boundary was designated the inlet with the maximum x-boundary was the outlet. The grid was supplied as part of the workshop. The grid was converted

to tetrahedrons within GlennICE. The 2D grid profile aligned with the sweep angle is shown in Figure 22. The final 3D grid consists of 14,564,096 tetrahedrons and 2,473,935 points.

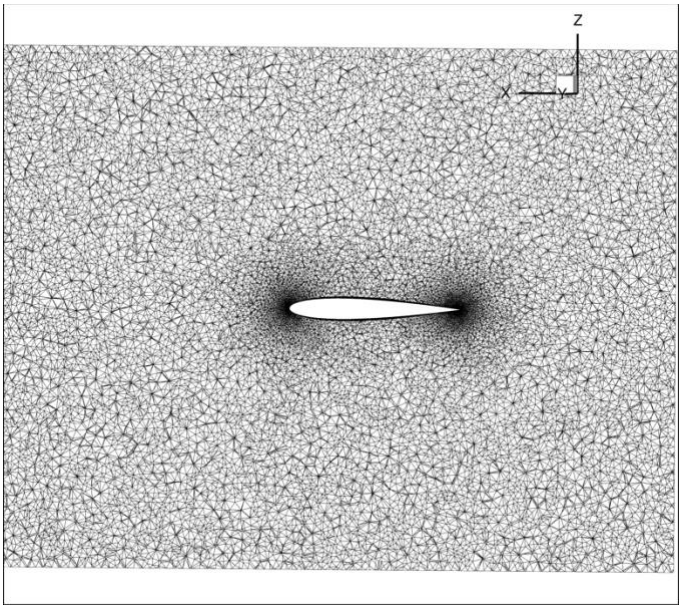

Figure 23 Grid Profile for the Swept NACA0012 Case

The flow solution was performed using FUN3D with a Shear Stress Transport turbulence model. Both flow solutions were generated used the following flow conditions: AOA = 0°, V_∞ = 115 m/s (224 knots), T= -8.3°C, P = 90321 Pa. The first flow solution used a constant wall temperature of 20°C and the second flow solution used a constant wall temperature of 30°C. The two different wall temperatures are used in GlennICE to compute the heat transfer coefficient. Icing conditions are LWC=0.5 g/m3 MVD=20.5 microns and an icing time of 17.7 minutes. Figure 24 shows a contour plot of Mach number for this case while Figure 25 shows pressure. Figure 26 shows surface pressure coefficient on the NACA0012 with comparison to experiment. The horizontal axis is the x-direction rotated 30° in order to compare with the experimental data. Figure 27 shows collection efficiency for this case. Figure 28 shows freezing fraction for this case. Figure 29 and Figure 30 show the roughness and augmentation to heat transfer respectively for $t_{r,max}$=0.004 and A=2.

Figure 31a shows the full span ice accretion from the experiment while Figure 31b shows the GlennICE result. The simulation assumes a uniform upstream cloud whereas the cloud in the IRT goes to zero at the floor. Since the geometry is a simple straight wing with a constant cross section, GlennICE produces an ice shape that looks similar to an extruded 2D shape even though the process is 3D. The cross-section ice shape looks like a standard double horn glaze ice shape from a 2D simulation and does not produce scallop ice shapes like the experiment. Since GlennICE does not produce ice scallops, it also needs to approximate the same cross-section area by employing an artificial ice density. The ice shape that was provided by the workshop for this condition was based on the maximum combined cross-section (MCCS). Lee [33] produced a technique that calculates the maximum combined cross-section (MCCS) as that shape qualitatively compares to the historical database which used pencil tracings to capture an ice shape. However, at any given cross-section, the actual ice shape profile can be smaller. Figure 32 shows the ice shape generated which is compared to MCCS ice shape from the scan from the experiment with ice density inputs of 200 kg/m^3 and 300 kg/m^3. These values were chosen to demonstrate that the final prediction is dependent on this value. Measurement of the voids created by scalloped ice shapes is the subject of ongoing research.

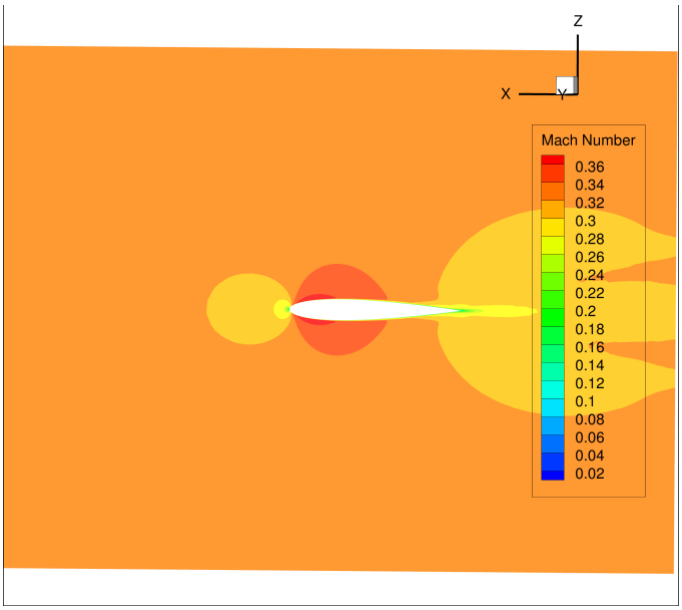

Figure 24 Mach Number Contours for Swept NACA0012 Case

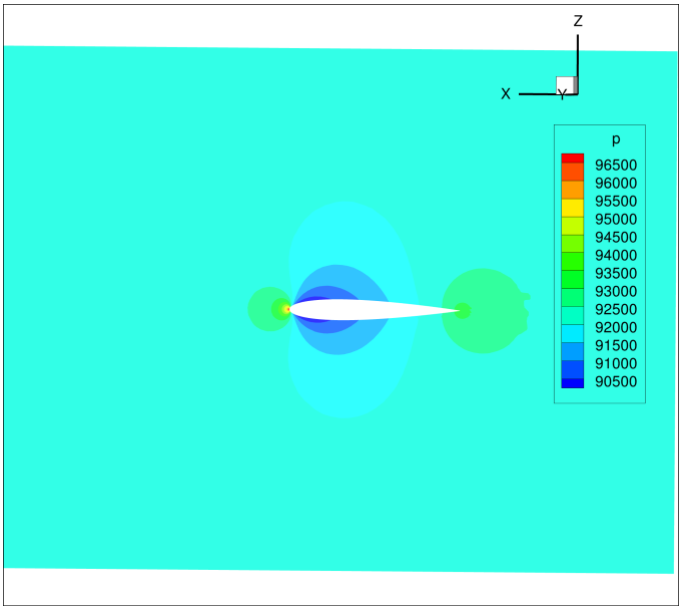

Figure 25 Pressure Contours for Swept NACA0012 Case

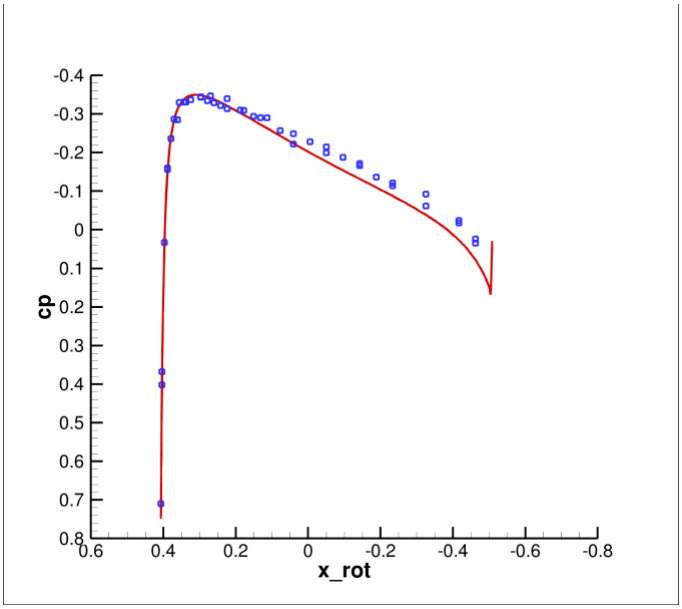

Figure 26 Surface Pressure Coefficient Compared to Experiment for Swept NACA0012 Case

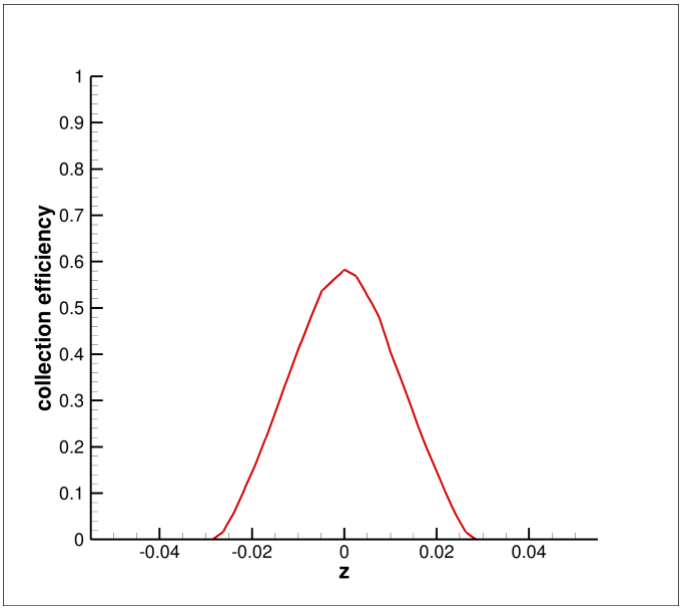

Figure 27 Collection Efficiency (β) for Swept NACA0012 Case

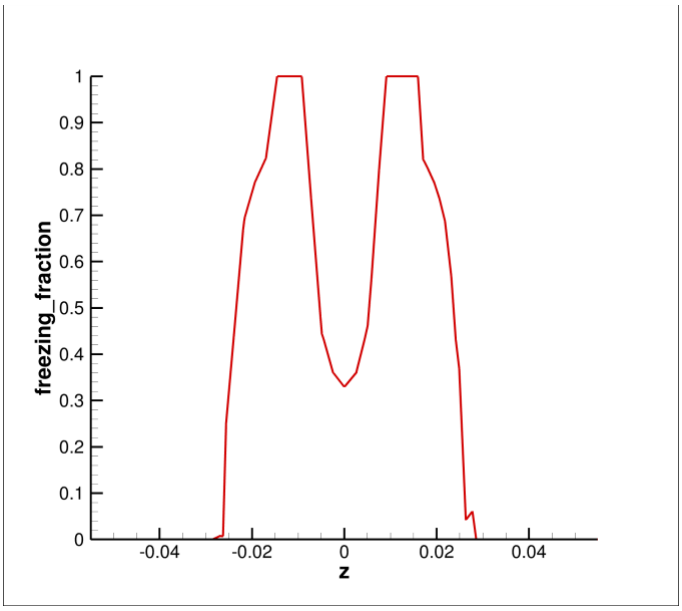

Figure 28 Freezing Fraction (η) for Swept NACA0012 Case

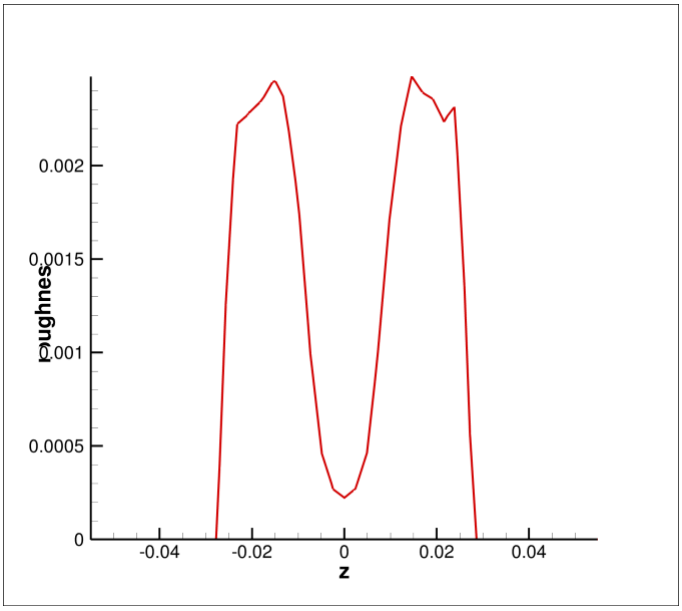

Figure 29 Roughness (R_q) Distribution Predicted for Swept NACA0012 Case

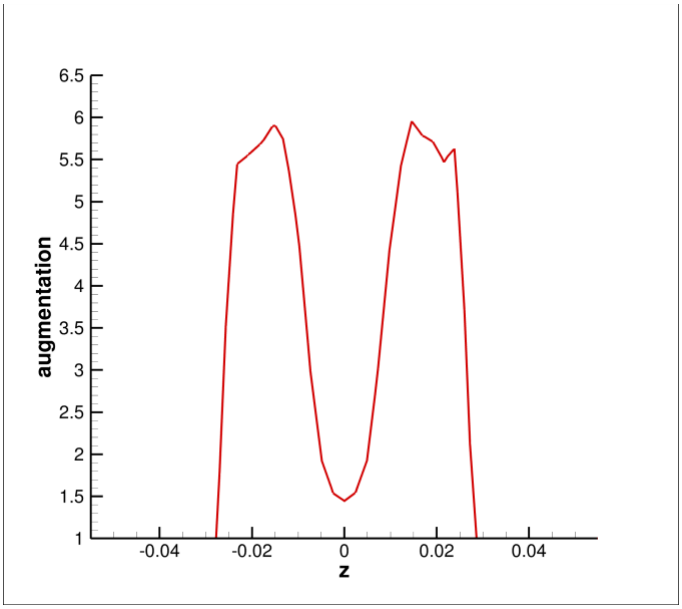

Figure 30 Heat Transfer Augmentation (htc_A/htc) Predicted for Swept NACA0012 Case

Experiment

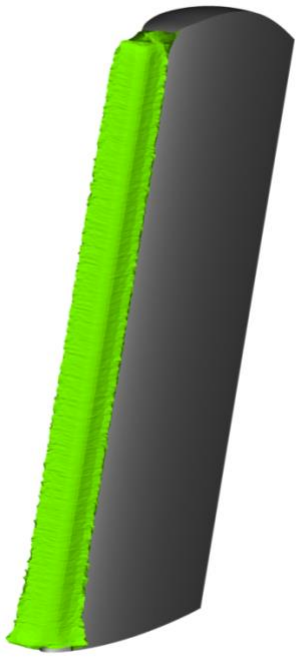

GlennICE

Figure 31 Ice Shapes for Swept NACA0012 Case

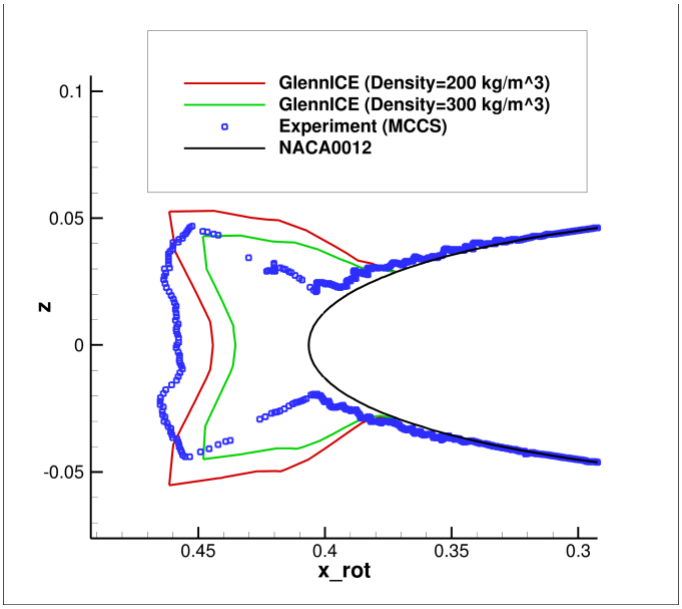

Figure 32 Ice Shapes at Two Ice Densities Compared to MCCS Ice Scan

V. Conclusion

A methodology has been presented for the GlennICE software, version 2.1. It involves reading a 3D flow solution and using that to calculate trajectories through the domain. A robust method for optimizing (minimizing) the number of trajectories required to obtain surface collection efficiency was presented here and in other papers. A method for obtaining heat transfer coefficients based on surface roughness was presented. The user-defined values for ideal rime limit and augmentation constant were chosen such that the ice shapes compared well with experiment. The water runback methodology was presented and the process for generating a full 3D iced surface was presented previously. Simulations were performed on three-dimensional geometries of interest to the icing community. Three test cases were selected for comparison to experimental data taken in the Icing Research Tunnel (IRT). The results showed comparable accuracy to the previous NASA software LEWICE3D. However, GlennICE is a fully 3D simulation whereas the LEWICE3D results are on 2D strips.

VI. Acknowledgements

The authors would like to acknowledge the support of the Advanced Air Transport Technology program for support for this research effort. The authors would also like to acknowledge the work of the rest of the Icing Branch, tunnel staff in the Icing Research Tunnel (IRT) and the Propulsion System Laboratory (PSL) for the validation data that is necessary to produce accurate simulations.

VII. References

[1] Wright, W. B. “Users Manual for LEWICE Version 3.2, NASA CR-2008-214255, Aug. 2008

[2] Bidwell, C. S., and Potapczuk, M. G., “Users Manual for the NASA Lewis Three-Dimensional Ice Accretion Code (LEWICE 3D), NASA TM-105974, Dec., 1993.

[3] “Technology readiness level” Wikipedia, Wikimedia Foundation, 29 September 2020, https://en.wikipedia.org/wiki/Technology_readiness_level

[4] Pueyo, A., Ozcer, I., and Baruzzi, G., "An Eulerian Approach with Mesh Adaptation for Highly Accurate 3D Droplet Dynamics Simulations," SAE Technical Paper 2019-01-2012, 2019, https://doi.org/10.4271/2019-01-2012.

[5] Villedieu, P., Trontin, P., Aouizerate, G., Bansmer, S. et al., "MUSIC-haic: 3D Multidisciplinary Tools for the Simulation of In-Flight Icing due to High Altitude Ice Crystals," *SAE Int. J. Adv. & Curr. Prac. in Mobility* 2(1):78-89, 2020, https://doi.org/10.4271/2019-01-1962.

[6] Al-Kebsi, A., Mose, R., and Hoarau, Y., "Multi-Step Ice Accretion Simulation Using the Level-Set Method," SAE Technical Paper 2019-01-1955, 2019, https://doi.org/10.4271/2019-01-1955.

[7] Durst, F. Miloievic, D. Schonung, B., “Eulerian and Lagrangian Predictions of Particulate Two-Phase Flows: A Numerical Study,” Appl. Mathematical Modelling, Vol. 8, Issue 2, April 1984, pp. 101-115.

[8] Fieldview, *Fieldview CFD Inc.*, https://www.fieldviewcfd.com/

[9] Tecplot, Tecplot Inc., https://tecplot.com

[10] Dormand, J. R., and P. J. Prince, “A Family of Embedded Runge-Kutta Formulae,” J. of Computational and Applied Mathematics, Vol. 6, Issue 1, March 1980 pp. 19-26

[11] E. Hairer, S.P. Norsett and G. Wanner, Solving Ordinary Differential Equations i. Nonstiff Problems. 2nd edition. Springer Series in Computational Mathematics, Springer-Verlag (1993).

[12] https://www.mathworks.com/help/matlab/ref/ode45.html

[13] https://octave.org/doc/interpreter/Matlab_002dcompatible-solvers.html#Matlab_002dcompatible-solvers

[14] Wright, W., Porter, C., Potapczuk, M., Galloway, E. and Rigby, D., “An Automated Refinement Process for Trajectory Methods in GlennICE,” AIAA Aviation Conference, June 2021.

[15] Wright, W., "Further Refinement of the LEWICE SLD Model", AIAA 2006-0464, Jan. 2006.

[16] Wright, W. B., Jorgenson, P. C. E., and Veres, J. P., “Mixed Phase Modeling in GlennICE with Application to Engine Icing”, AIAA-2010-810932.

[17] Bartkus. T. P., and Struk, P. M., “Comparisons of CFD Simulations of Icing Wind Tunnel Clouds with Experiments Conducted at the NASA Propulsion Systems Laboratory,” AIAA 2020-2832.

[18] Aupoix B. A general strategy to extend turbulence models to rough surfaces: application to Smith’s k–L model. Trans ASME, J Fluids Eng 2007;129:1245–54.

[19] Langtry, R., Menter, F., 2009. Correlation-based transition modelling for unstructured parallelized computational fluid dynamics codes. AIAA J. 47, 2894–2906.

[20] Roberts, I., "Motivation, Development and Verification of a Rapid 3D Lagrangian Impingement Code - Trajectory and Catch 3D+ (TAC3D+)," SAE Technical Paper 2019-01-2011, 2019, https://doi.org/10.4271/2019-01-2011.

[21] Ozcer, I., Baruzzi, G., Reid, T., Habashi, W. et al., “FENSAPICE: Numerical Prediction of Ice Roughness Evolution, and its Effects on Ice Shapes,” SAE Technical Paper 2011-38-0024, 2011, doi:10.4271/2011-38-0024.

[22] Eca., L., and Hoekstra. M., “Numerical aspects of including wall roughness effects in the SST k–x eddy-viscosity turbulence model,” Computers & Fluids 40 (2011) 299–314

[23] Langel, C. M., et. al., “A Computational Approach to Simulating the Effects of Realistic Surface Roughness on Boundary Layer Transition, “52nd Aerospace Sciences Meeting, AIAA SciTech Forum, 2014.

[24] Ge, X., and Durbin, P. A., “An intermittency model for predicting roughness induced transition,” International Journal of Heat and Fluid Flow 54 (2015) 55–64

[25] Min, S., Son, C. and Ye, K., “Extension of Surface Roughness Model for Navier-Stokes Equation Based Aircraft Icing Code,” Tenth International Conference on Computational Fluid Dynamics (ICCFD10), Barcelona, Spain, July 9-13, 2018

[26] Fortin, G., “Equivalent Sand Grain Roughness Correlation for Aircraft Ice Shape Predictions,” SAE Technical Paper 2019-01-1978, 2019.

[27] McClain, S. T., Vargas, M,. Tsao, J., and Broeren, A. P., “A Model for Ice Accretion Roughness Evolution and Spatial Variations,” AIAA 2021-2641.

[28] Porter, C. E., and Rigby, D. L., “Three Dimensional Surface Redefinition Method for Computational Ice Accretion Solvers,” AIAA Aviation Virtual Conference, 2020.

[29] Wright, W. B., “Validation Methods and Results for a Two-Dimensional Ice Accretion Code,: J. of Aircraft, Vol. 35, No, 5, Sept. 1999.

[30] Proceeds of the 1st AIAA Ice Prediction Workshop, https://icepredictionworkshop.wordpress.com, 2021.

[31] Pointwise, *Pointwise Inc.*, https://www.pointwise.com/

[32] Ansys-CFX, *Ansys Inc.*, Canonsburg, PA; software available at https://www.ansys.com

[33] Lee, S., Broeren, A.P., and Potapczuk, M.G., “Comparison of Ice Shapes on Full Chord and Truncated Swept Wing Models,” AIAA-2021-2679.